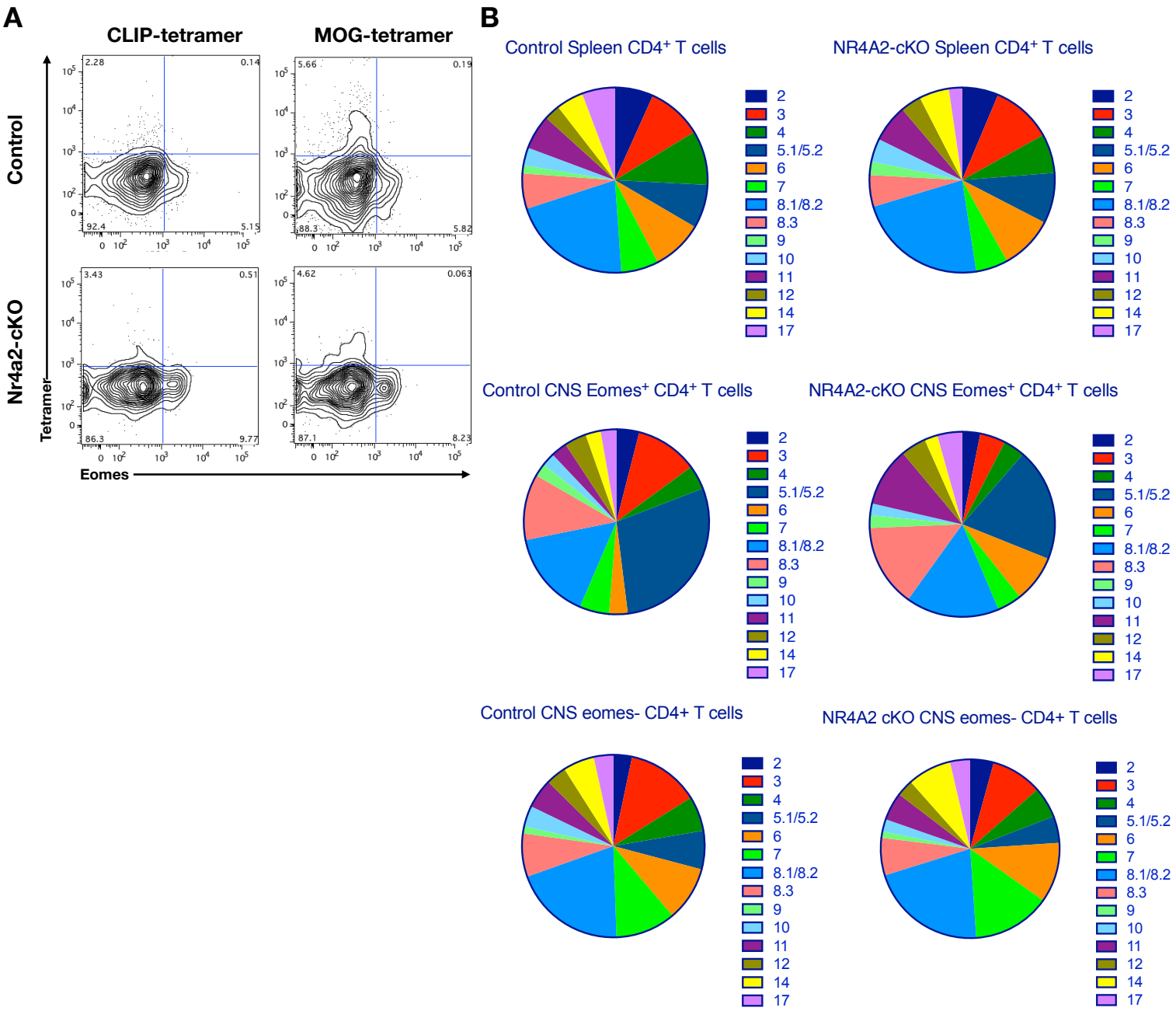
A
CLIP-tetramer
MOG-tetramer
Control
Nr4a2-cKO
Tetramer
Eomes
2.28
0.14
92.4
5.15
5.66
0.19
88.3
5.82
3.43
0.51
86.3
9.77
4.62
0.063
87.1
8.23
B
Control Spleen CD4+ T cells
NR4A2-cKO Spleen CD4+ T cells
Control CNS Eomes+ CD4+ T cells
NR4A2-cKO CNS Eomes+ CD4+ T cells
Control CNS eomes- CD4+ T cells
NR4A2 cKO CNS eomes- CD4+ T cells
2
3
4
5.1/5.2
6
7
8.1/8.2
8.3
9
10
11
12
14
17

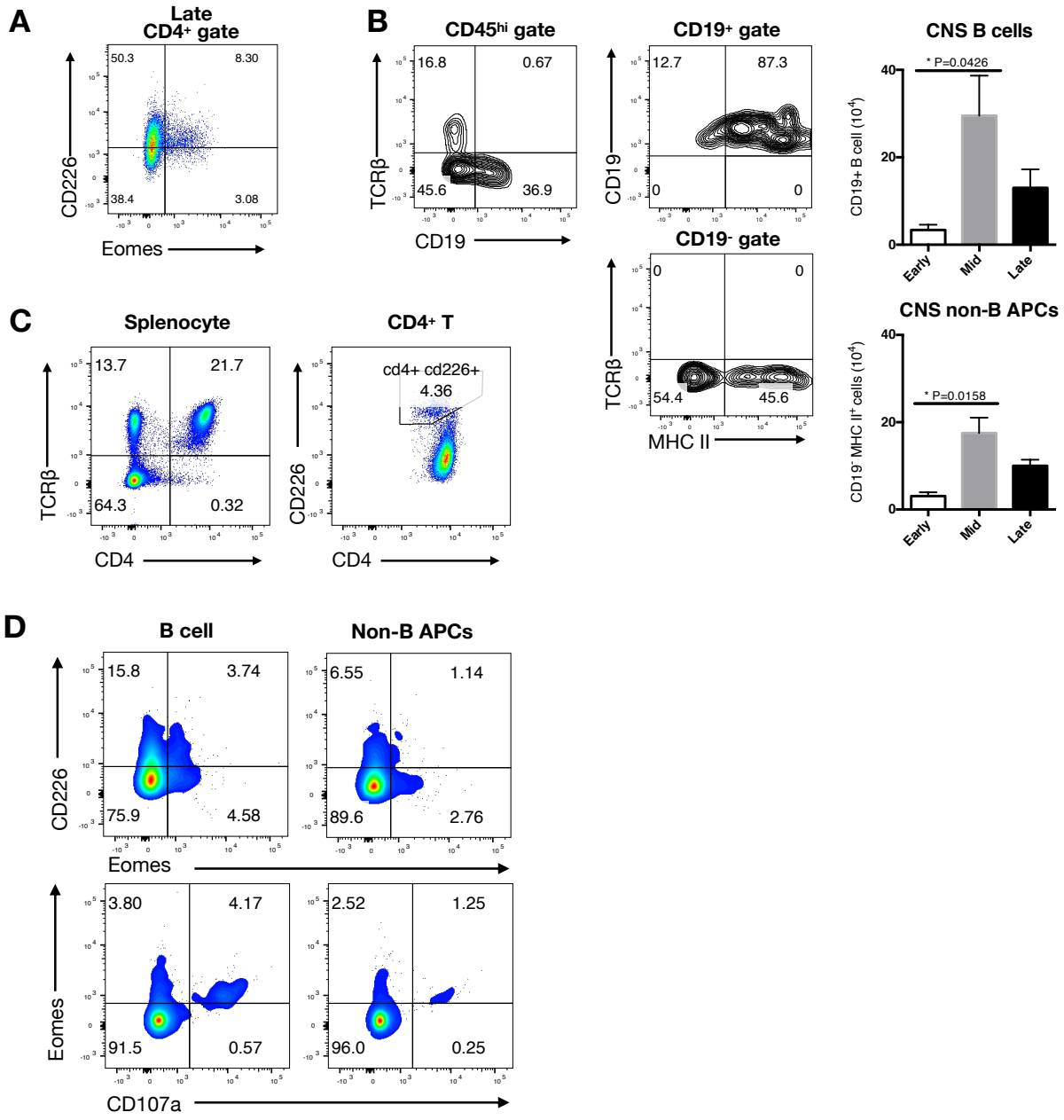
A
Late
CD4+ gate
50.3
8.30
38.4
3.08
CD226
Eomes
B
CD45hi gate
16.8
0.67
45.6
36.9
TCRβ
CD19
CD19+ gate
12.7
87.3
0
0
CD19
CD19- gate
0
0
54.4
45.6
TCRβ
MHC II
CNS B cells
* P=0.0426
CD19+ B cell (10^4)
40
20
0
Early
Mid
Late
CNS non-B APCs
* P=0.0158
CD19- MHC II+ cells (10^4)
40
20
0
Early
Mid
Late
C
Splenocyte
13.7
21.7
64.3
0.32
TCRβ
CD4
CD4+ T
cd4+ cd226+
4.36
CD226
CD4
D
B cell
Non-B APCs
15.8
3.74
75.9
4.58
6.55
1.14
89.6
2.76
CD226
Eomes
3.80
4.17
91.5
0.57
2.52
1.25
96.0
0.25
Eomes
CD107a

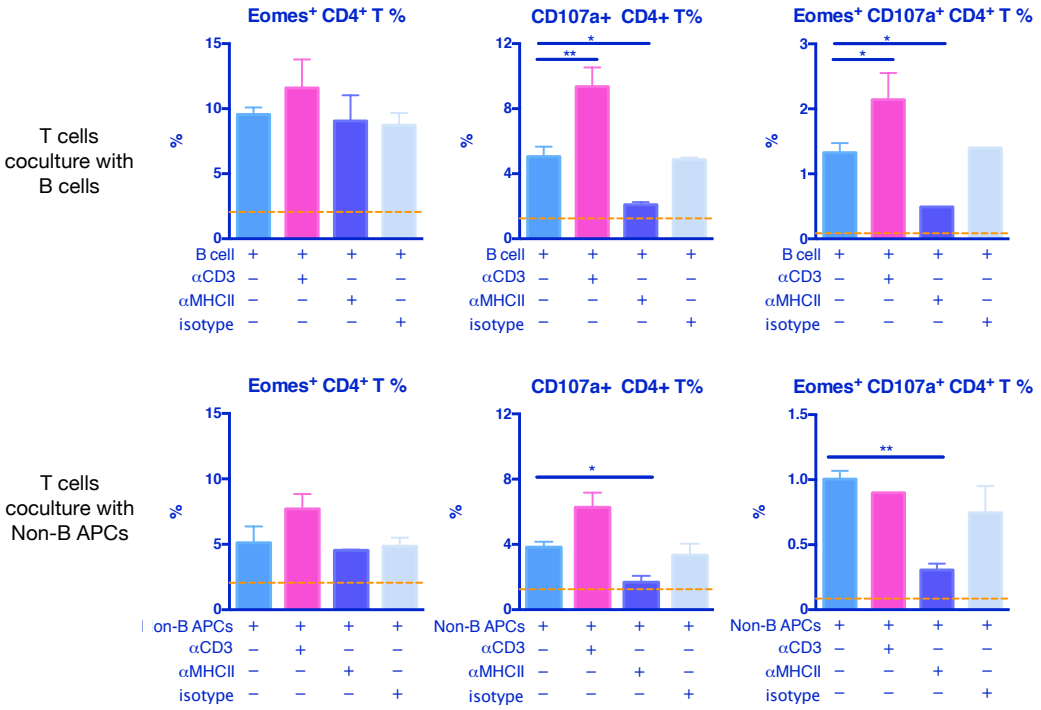
T cells coculture with B cells
Eomes+ CD4+ T %
CD107a+ CD4+ T%
Eomes+ CD107a+ CD4+ T %
%
B cell
αCD3
αMHCII
isotype
T cells coculture with Non-B APCs
Non-B APCs

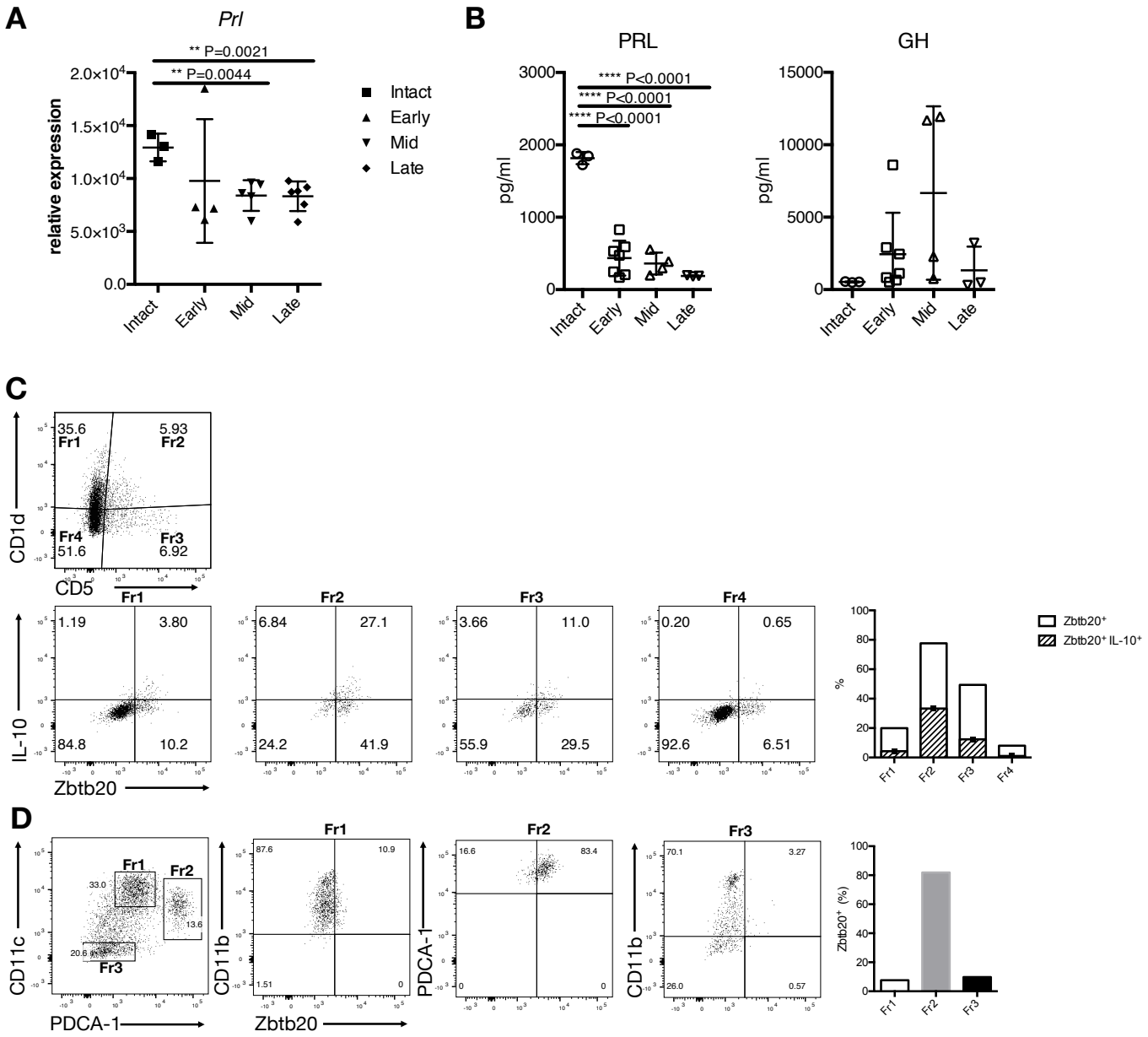
A
Prl
** P=0.0021
** P=0.0044
relative expression
2.0x10^4
1.5x10^4
1.0x10^4
5.0x10^3
0.0
Intact
Early
Mid
Late
B
PRL
GH
**** P<0.0001
**** P<0.0001
**** P<0.0001
pg/ml
3000
2000
1000
0
15000
10000
5000
C
CD1d
CD5
35.6
Fr1
5.93
Fr2
Fr4
51.6
Fr3
6.92
IL-10
Zbtb20
1.19
3.80
84.8
10.2
6.84
27.1
24.2
41.9
3.66
11.0
55.9
29.5
0.20
0.65
92.6
6.51
%
Zbtb20+
Zbtb20+ IL-10+
D
CD11c
PDCA-1
33.0
13.6
20.6
CD11b
Zbtb20
87.6
10.9
1.51
0
16.6
83.4
70.1
3.27
26.0
0.57
Zbtb20+ (%)

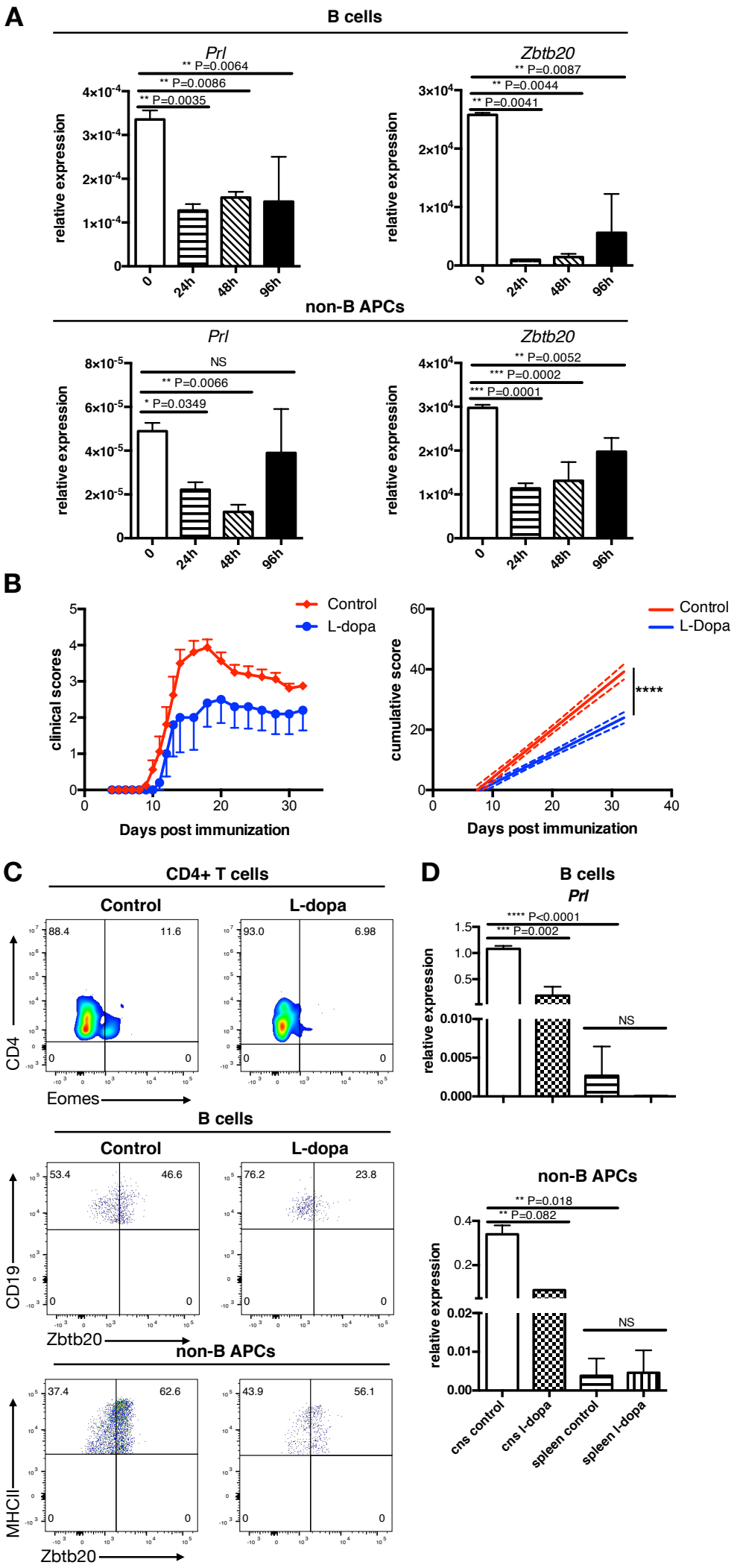
A
B cells
Prl
** P=0.0064
** P=0.0086
** P=0.0035
relative expression
4x10-4
3x10-4
2x10-4
1x10-4
0
0
24h
48h
96h
Zbtb20
** P=0.0087
** P=0.0044
** P=0.0041
3x10^4
2x10^4
1x10^4
non-B APCs
Prl
NS
** P=0.0066
* P=0.0349
8x10-5
6x10-5
4x10-5
2x10-5
Zbtb20
** P=0.0052
*** P=0.0002
*** P=0.0001
B
Control
L-dopa
clinical scores
Days post immunization
cumulative score
****
C
CD4+ T cells
Control
L-dopa
88.4
11.6
93.0
6.98
CD4
Eomes
B cells
53.4
46.6
76.2
23.8
CD19
Zbtb20
non-B APCs
37.4
62.6
43.9
56.1
MHCII
Zbtb20
D
B cells
Prl
**** P<0.0001
*** P=0.002
NS
relative expression
non-B APCs
** P=0.018
** P=0.082
cns control
cns l-dopa
spleen control
spleen l-dopa

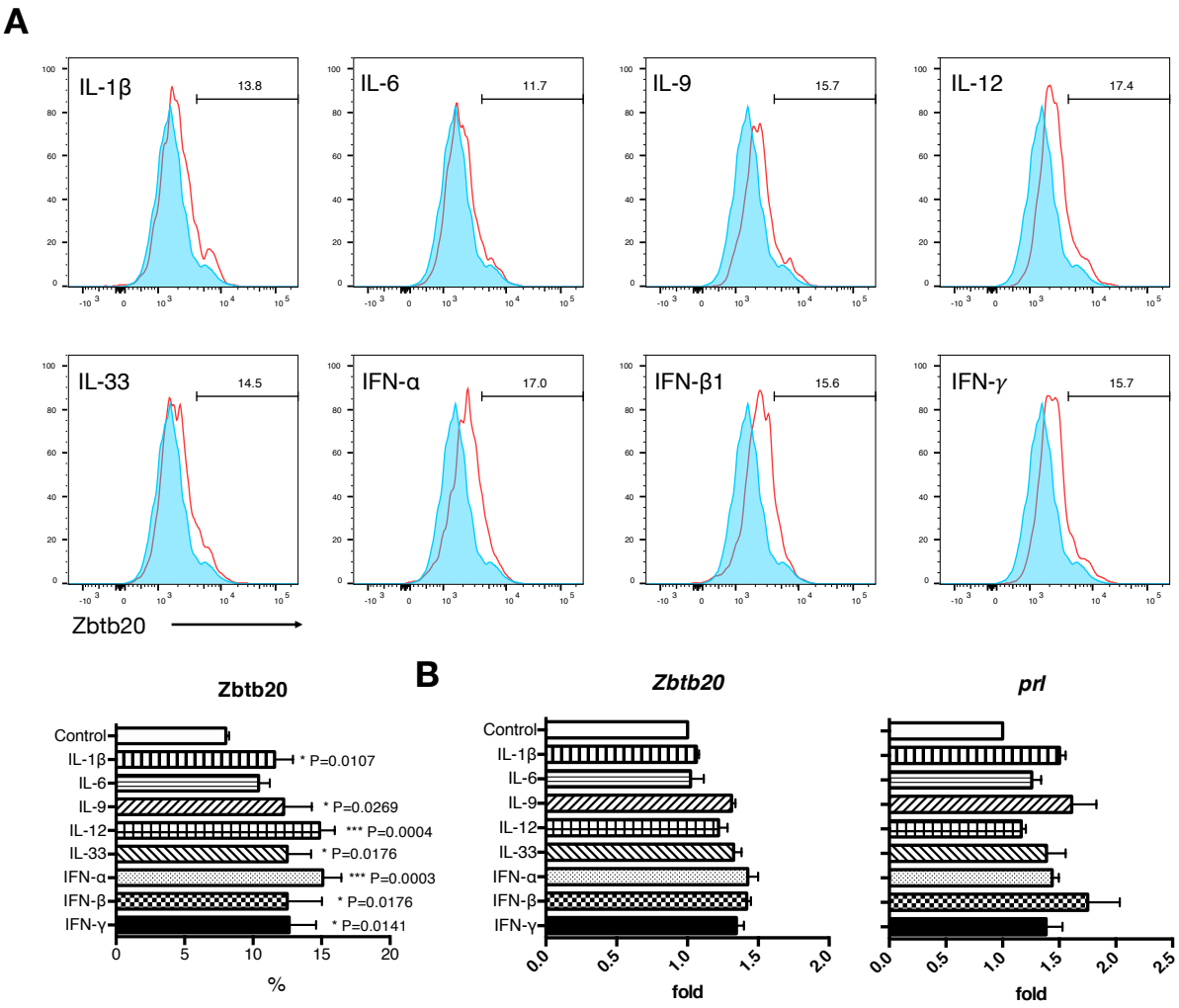
A
IL-1β
13.8
IL-6
11.7
IL-9
15.7
IL-12
17.4
IL-33
14.5
IFN-α
17.0
IFN-β1
15.6
IFN-γ
15.7
Zbtb20
B
Zbtb20
Control
IL-1β
IL-6
IL-9
IL-12
IL-33
IFN-α
IFN-β
IFN-γ
* P=0.0107
* P=0.0269
*** P=0.0004
* P=0.0176
*** P=0.0003
* P=0.0176
* P=0.0141
%
Zbtb20
fold
prl
fold

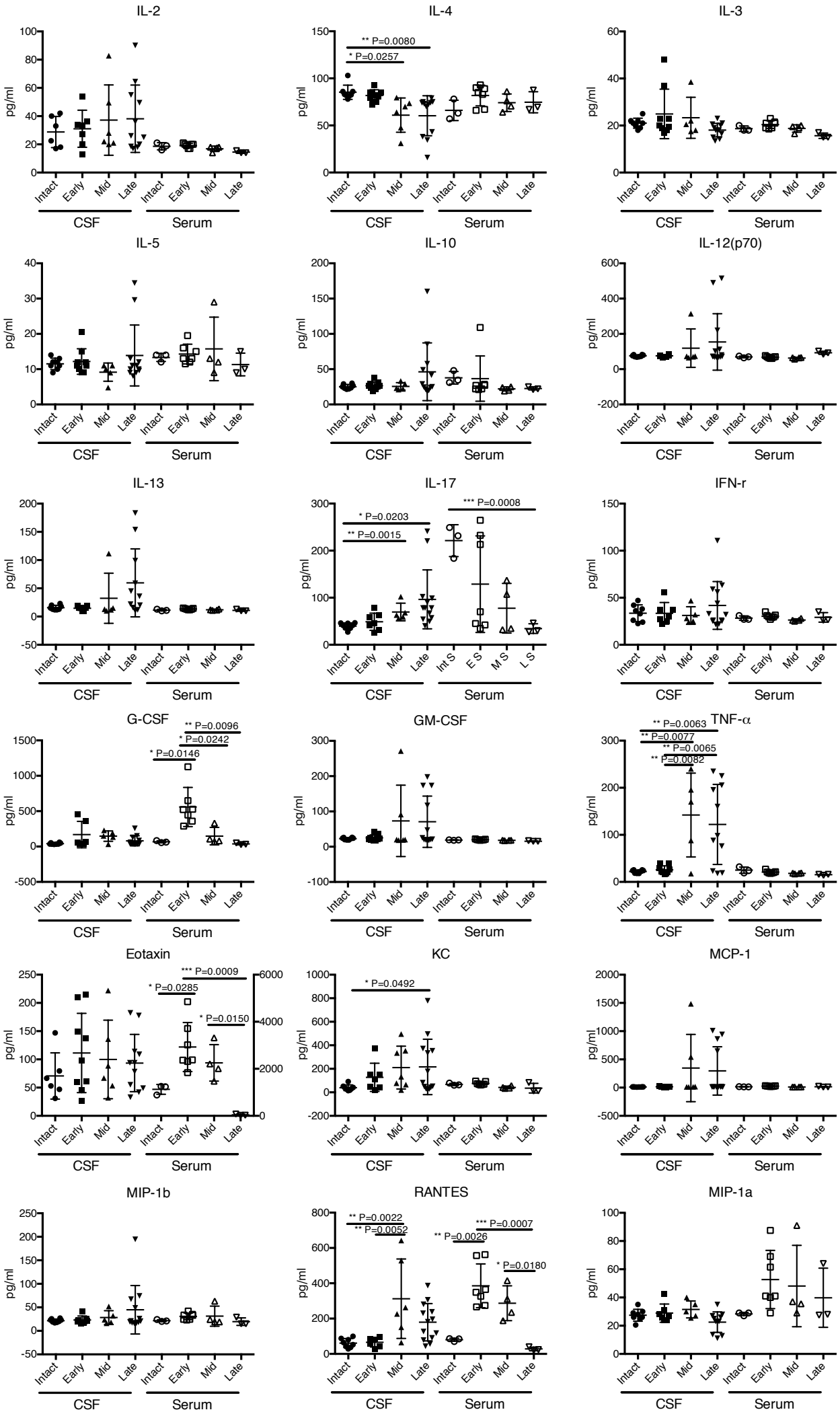
IL-2
IL-4
IL-3
IL-5
IL-10
IL-12(p70)
IL-13
IL-17
IFN-r
G-CSF
GM-CSF
TNF-α
Eotaxin
KC
MCP-1
MIP-1b
RANTES
MIP-1a
pg/ml
Intact
Early
Mid
Late
CSF
Serum
Int S
E S
M S
L S
** P=0.0080
* P=0.0257
* P=0.0203
** P=0.0015
*** P=0.0008
** P=0.0096
* P=0.0242
* P=0.0146
** P=0.0063
** P=0.0077
** P=0.0065
** P=0.0082
*** P=0.0009
* P=0.0285
* P=0.0150
* P=0.0492
** P=0.0022
** P=0.0052
** P=0.0026
*** P=0.0007
* P=0.0180

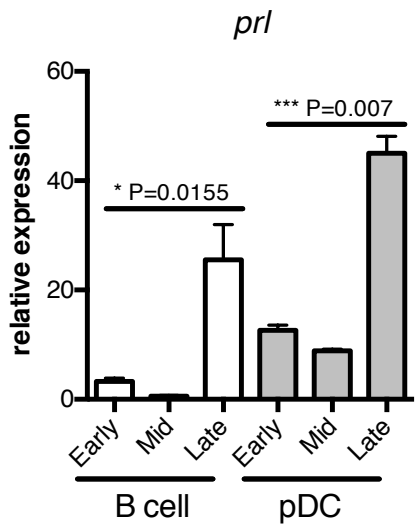
prl
relative expression
60
40
20
0
* P=0.0155
*** P=0.007
Early
Mid
Late
Early
Mid
Late
B cell
pDC

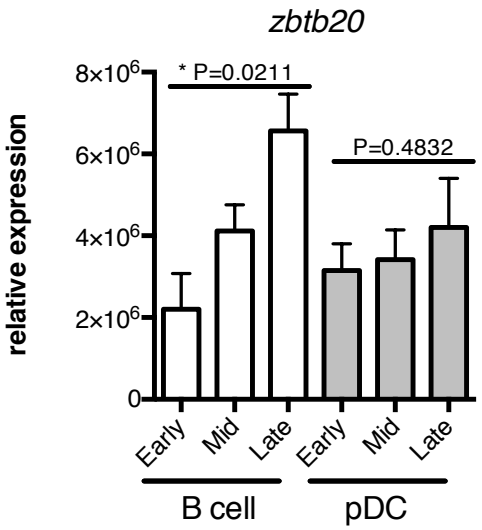
zbtb20
relative expression
8×10^6
6×10^6
4×10^6
2×10^6
0
* P=0.0211
P=0.4832
Early
Mid
Late
Early
Mid
Late
B cell
pDC

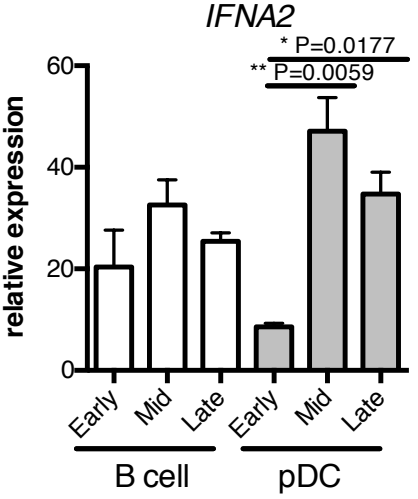
IFNA2
relative expression
60
40
20
0
* P=0.0177
** P=0.0059
Early
Mid
Late
Early
Mid
Late
B cell
pDC

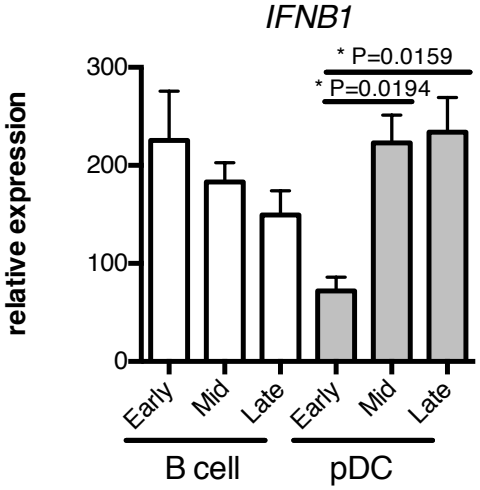
IFNB1
relative expression
300
200
100
0
* P=0.0159
* P=0.0194
Early
Mid
Late
Early
Mid
Late
B cell
pDC

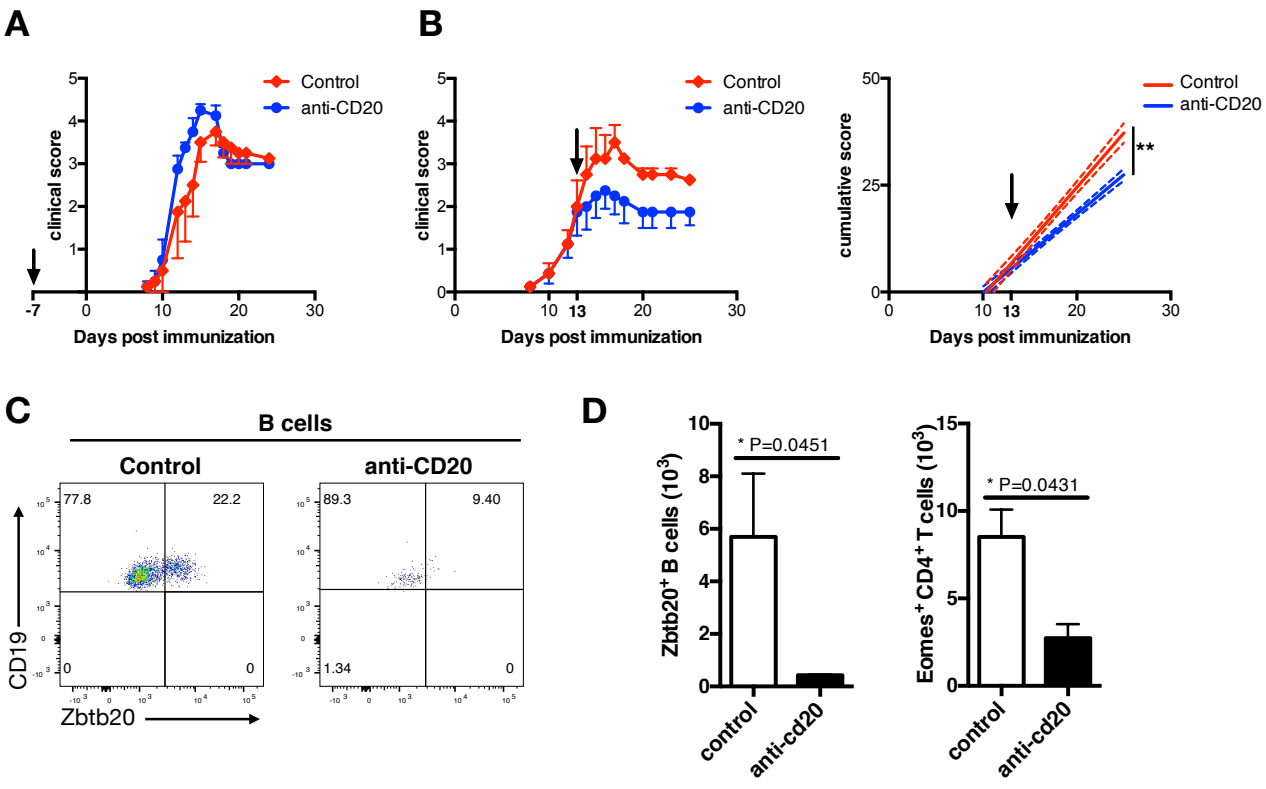
A
B
Control
anti-CD20
clinical score
Days post immunization
cumulative score
**
C
B cells
Control
anti-CD20
77.8
22.2
0
0
89.3
9.40
1.34
0
CD19
Zbtb20
D
* P=0.0451
Zbtb20+ B cells (10^3)
control
anti-cd20
* P=0.0431
Eomes+ CD4+ T cells (10^3)
control
anti-cd20

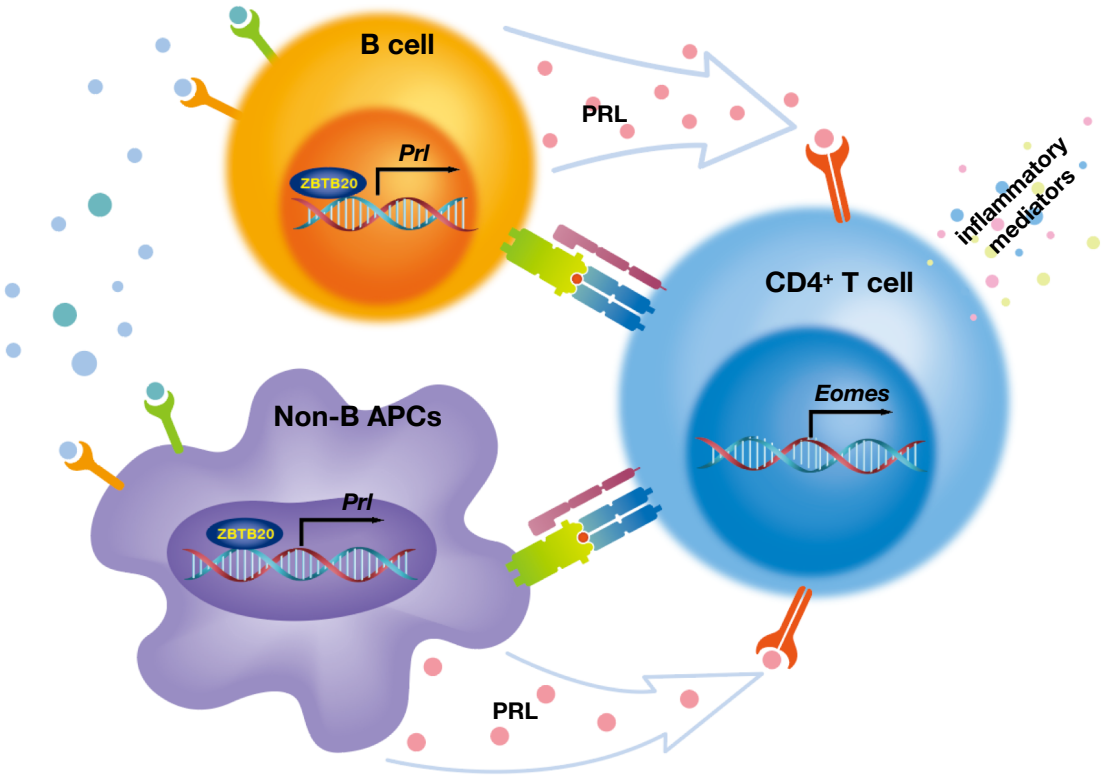
B cell
Prl
ZBTB20
PRL
inflammatory mediators
CD4+ T cell
Eomes
Non-B APCs
Prl
ZBTB20
PRL

	GO term	enrichment (P-value)
biological process	immune system process (GO:0002376)	8.12E-12
	positive regulation of immune system process (GO:0002684)	6.69E-08
	response to external stimulus (GO:0009605)	1.49E-07
	regulation of immune system process (GO:0002682)	2.25E-07
	response to other organism (GO:0051707)	3.36E-07
	response to external biotic stimulus (GO:0043207)	3.57E-07
	response to oxygen-containing compound (GO:1901700)	7.19E-07
	response to biotic stimulus (GO:0009607)	8.35E-07
	leukocyte migration (GO:0050900)	1.50E-06
	immune response (GO:0006955)	1.67E-06
	response to bacterium (GO:0009617)	2.44E-06
	defense response (GO:0006952)	9.52E-06
	positive regulation of response to stimulus (GO:0048584)	1.03E-04
	defense response to bacterium (GO:0042742)	1.23E-04
	antimicrobial humoral response (GO:0019730)	1.72E-04
	defense response to other organism (GO:0098542)	2.06E-04
	modification of morphology or physiology of other organism (GO:0035821)	2.84E-04
	regulation of cell proliferation (GO:0042127)	1.09E-03
	leukocyte chemotaxis (GO:0030595)	1.11E-03
	multi-organism process (GO:0051704)	1.26E-03
	positive regulation of biological process (GO:0048518)	1.85E-03
	regulation of response to stimulus (GO:0048583)	2.15E-03
	response to stimulus (GO:0050896)	2.36E-03
	cell migration (GO:0016477)	2.55E-03
	antimicrobial humoral immune response mediated by antimicrobial peptide (GO:0061844)	2.69E-03
	positive regulation of leukocyte migration (GO:0002687)	3.11E-03
	response to stress (GO:0006950)	3.21E-03
	disruption of cells of other organism (GO:0044364)	3.28E-03
	killing of cells of other organism (GO:0031640)	3.28E-03
	positive regulation of cellular process (GO:0048522)	3.44E-03
	regulation of response to external stimulus (GO:0032101)	4.63E-03
	cell chemotaxis (GO:0060326)	4.89E-03
	regulation of multicellular organismal process (GO:0051239)	5.05E-03
	tissue remodeling (GO:0048771)	5.38E-03
	positive regulation of locomotion (GO:0040017)	5.48E-03
	positive regulation of cell migration (GO:0030335)	6.19E-03
	negative regulation of biological process (GO:0048519)	6.73E-03
	humoral immune response (GO:0006959)	7.14E-03
	modification of morphology or physiology of other organism involved in symbiotic interaction (GO:0051817)	8.23E-03
	interspecies interaction between organisms (GO:0044419)	9.84E-03
	positive regulation of cell motility (GO:2000147)	9.95E-03
molecular function	glycosaminoglycan binding (GO:0005539)	7.47E-06
	receptor binding (GO:0005102)	3.14E-05
	cytokine activity (GO:0005125)	1.74E-03
	heparin binding (GO:0008201)	2.80E-03
	chemokine activity (GO:0008009)	6.16E-03
component complete	extracellular space (GO:0005615)	6.76E-10
	extracellular region part (GO:0044421)	3.11E-09
	extracellular region (GO:0005576)	2.49E-08
	cell surface (GO:0009986)	1.00E-06
	vesicle (GO:0031982)	6.08E-05
	extracellular matrix (GO:0031012)	3.46E-03
	cytoplasmic vesicle (GO:0031410)	5.14E-03
	intracellular vesicle (GO:0097708)	5.49E-03

SI Appendix, Figure 1. MOG tetramer and V TCR analysis for Eomes$^+$ Th cells

NR4A2 cKO and control WT B6 mice (Control) were immunized with MOG_{35-55} for inducing EAE. During the late phase of EAE, single cell suspensions were prepared from spleen and the CNS tissue of these mice for flow cytometer analysis. (**A**) The cells isolated from the CNS were treated with neuraminidase, and then stained with MOG_{35-55}/MHC class II-tetramer at room temperature. Human-CLIP/MHC class II tetramer was used as a staining control. Cells were co-stained with antibodies against surface markers, before fixation and intracellular staining for Eomes. n=5 mice per group. (B) Cells were surface stained with the mouse V TCR screen panel kit (BD Biosciences). Then intracellular staining was performed with antibodies against Eomes. Percentages of each V subset among Eomes$^+$ and Eomes$^-$ CD4$^+$ T cells are summarized and shown in pie graphs. The pie graphs in the middle demonstrate the biased usage for V5.1/5.2 and V8.3 observed in lymphocytes from late EAE CNS lesions as compared to those from naïve spleen cells (upper) and Eomes$^-$ cells (bottom).

SI Appendix, Figure 2. Eomes$^+$ Th cells, B cells and non-B cell APCs at early, middle and late time points of EAE

(**A**) Expressions of CD226 and Eomes in CNS CD4$^+$ T cells isolated from late phase of EAE. Results are shown by FACS plot. (**B**) Scheme of CNS APCs sorting. Pooled CNS APCs were isolated from EAE mice at different stages. CNS CD19$^+$ B cells and CNS CD19$^-$CD45^{hi} MHC II$^+$ non-B APCs were sorted by FACS sorting (left). Cell number was counted (right). Error bars show mean ± SD. P value is shown in figures; One-way ANOVA test with Dunnett's multiple comparisons test. (**C**) The gating strategy for purifying CD4$^+$CD226$^+$ T cells from naïve spleen cells. (**D**) WT B6 mice were subcutaneously immunized with MOG_{35-55} peptide emulsified in CFA plus i.p. pertussis toxin for inducing EAE. CNS myeloid APCs were isolated at late time point indicated in Fig 1A. From the isolated cells, CD19$^+$ B cells and CNS CD19$^-$CD45^{hi} MHC II$^+$ non-B APCs were purified by FACS sorting, and then co-cultured with FACS sorted splenic CD4$^+$ T cells derived from congenic naive mice in the presence of FITC conjugated anti-CD107a antibody. After 8 h culture, cells were intracellularly stained for expression of Eomes. FACS plots show the expression of CD226, Eomes and CD107a surface trapping in CD4$^+$ T cells co-cultured with CNS B cells (left half) or CNS non-B APCs (right half).

SI Appendix, Figure 3. Requirement for MHC II-TCR interactions in the induction of cytotoxic CD107a$^+$Eomes$^+$ Th cells

FACS-sorted CNS B cells and non-APCs from EAE mice were cocultured with FACS-sorted splenic CD226$^+$CD4$^+$ T cells from naïve congenic mice. Indicated antibodies were added into culture medium. Bar graphs demonstrate the summarized percentage values for Eomes$^+$ cells (%), CD107$^+$ cells (%) and Eomes$^+$CD107a$^+$ cells (%) among CD4$^+$ T cells after cultured with B cells (top half) or non-B cell APCs (bottom). Orange dashed lines in each bar graph represent the basal values of uncultured CD226$^+$ CD4$^+$ T cells. Error bars represent the mean ± SD values. n = 5 mice in each group; * $p<0.05$; ** $p<0.01$; One-way ANOVA test with multiple comparisons test.

SI Appendix, Figure 4. Prolactin/Zbtb20 expression in the pituitary glands and subpopulations of the CNS APC

(**A**) Pituitary glands were dissected from intact or EAE mice. Total RNA was isolated and the expression levels of Prl were determined by qRT-PCR. Error bars show mean ± SD. P value is shown in figures; One-way ANOVA test with Dunnett's multiple comparisons test. (**B**) Protein levels of PRL and GH in the serum of EAE mice were determined by Luminex system (see also Material and Method). Error bars show mean ± SD. P value is shown in figures; One-way ANOVA test with Dunnett's multiple comparisons test. (**C**) CNS B cells derived from late EAE lesions were cultured in the presence of 10 μg/ml LPS with Golgi-plug for 6 hours. After setting the B cell gate, cells were divided into four fractions by CD1d and CD5 expression. Expression levels of IL-10 and Zbtb20 from each fraction are shown with FACS plots. The proportions of Zbtb20$^+$ and Zbtb20$^+$ IL-10$^+$ cells are shown using bar graph (right). (**D**) Freshly isolated CNS non-B cell APCs cells from late EAE were stained and analyzed by FACS. Cells were divided into three fractions based on CD11c and PDCA-1 expression, and expression level of Zbtb20 from each fraction is shown with FACS plots (left). The proportions of Zbtb20$^+$ cells (%) are shown using bar graph (right).

SI Appendix, Figure 5. Dopamine blocks induction of Zbtb20/prolactin in the CNS APCs
(**A**) Mixed populations of CNS APCs were isolated from late EAE mice. CNS $CD19^+$ B cells (top) and CNS $CD19^-CD45^{hi}$ MHC II^+ non-B APCs (bottom) were purified by FACS sorting, cultured in the absence or presence of dopamine for indicated time points. Cultured cells were then harvested and committed qRT-PCR for *Prl* and *Zbtb20* expression. Error bars show mean ± SD. P value is shown in figures; One-way ANOVA test with Dunnett's multiple comparisons test. **(B)** WT B6 mice were immunized with MOG_{35-55} peptide emulsified in CFA and boosted by i.p. pertussis toxin. L-dopa or control solution (Control) was administered i.p. on day 4 post immunization. Afterwards, the injections were repeated every other day. Clinical EAE scores are shown with error bars representing SEM. In the right panel, solid lines represent cumulative disease score, whereas dash lines indicate the 95% confidence intervals. ****, $p<0.001$; linear regression analysis. (**C**) $CD4^+$ T cells, B cells and non-B APCs were isolated from EAE lesions of the control and L-dopa-treated mice. They were intracellularly stained for Eomes or Zbtb20. Flow cytometry plots show representative data from two independent experiments. (**D**) *Prl* levels in B cells and non-B cell APCs from CNS and spleen were determined by qRT-PCR. Error bars show mean ± SD. P value is shown in figures; One-way ANOVA test with Dunnett's multiple comparisons test.

SI Appendix, Figure 6. Cytokines regulating expression of Zbtb20 are differentially altered during the course of EAE. Splenic $CD19^+$ B cells were isolated and purified by FACS sorting. To maintain viability, all B cells were cultured in the presence of LPS, with or without indicated cytokines, for 24 h. (**A**) Cultured cells were then intracellularly stained to detect the expression of Zbtb20 and subjected to flow cytometric analysis. Error bars show mean ± SD. P value is shown in figures; One-way ANOVA test with Dunnett's multiple comparisons test. (**B**) In parallel, qRT-PCR was performed for measuring the expression of *Zbtb20* and *Prl*. Expression levels were compared with the control and were expressed in terms of fold changes. FACS staining plots are representative of two independent experiments. The control (without cytokine) is represented by a solid profile, and stimulation with cytokines is represented by the thin line.

SI Appendix, Figure 7. Protein levels of cytokines and chemokines in mouse CSF and serum.
Protein levels of cytokines and chemokines in CSF and serum derived from intact or EAE mice were determined by Luminex system. Error bars show mean ± SD. P value is shown in figures; One-way ANOVA test with Dunnett's multiple comparisons test.

SI Appendix, Figure 8. Expression of IFNA2 and IFNB1 as well as prl and zbtb20 in CNS B cells, pDC and microglia. CNS CD19 B cells, PDCA-1^+ $B220^+$ pDC, and $CD45^{int}$ $CD11b^+$ microglia were isolated from early, mid, and late phase of EAE by FACS Aria. Expression levels of *prl*、*zbtb20, IFNA2, and IFNB1* were quantified by qRT-PCR. Error bars show mean ± SD. P value is shown in figures; One-way ANOVA test with Dunnett's multiple comparisons test.

SI Appendix, Figure 9. B cells depletion inhibits late EAE disease
WT B6 mice were immunized with MOG_{35-55} peptide emulsified in CFA and boosted by i.p. pertussis toxin. Anti-CD20 antibodies or control IgG was i.v. administrated on day -7 prior to immunization (**A**) or day 13 post immunization (**B-D**). (**A, B**) Clinical EAE scores are shown with error bars representing SEM. In the right panel, solid lines represent cumulative disease scores, and dash lines indicate the 95% confidence intervals. **, $p=0.0026$; linear regression analysis. (**C**) Freshly isolated CNS B cells and $CD4^+$ T cells were intracellularly stained for Zbtb20 and Eomes respectively. Flow cytometry plots show representative data from two independent experiments. (**D**) Summary of exact number of $Eomes^+$ $CD4^+$ T cells and $Zbtb20^+$ B cells. Error bars show mean ± SD. P value is shown in figures; student's t-test.

SI Appendix, Figure 10. Scheme of our hypothesis
See the text.

SI Appendix, Table 1. GO analysis of the gene up-regulated in CNS B cells during late EAE disease
The genes are firstly filtered as 1% high variance in all annotated genes, classified as up-regulated expression in B cell from late EAE, then applied to GO analysis with PANTHER.